NUMERICAL INVESTIGATION OF AXIAL FANS IN SERIAL CONNECTION

Gabriel AXTMANN , Michael SCHMITZ , Wolfgang LAUFER

ebm-papst St. Georgen GmbH & Co.KG, 78112 Hermann-Papst-Straße 1, 78112 St. Georgen im Schwarzwald, Germany

SUMMARY

The aerodynamic performance of two identical axial compact fans in a serial arrangement is studied. These arrangements are used in the telecom industry to increase overall pressure levels [1] and keeping redundancy and exchangeability of the components. Typically, two identical axial fans are used sometimes with flow straighteners in between. In this study, a two-stage set-up of identical fans is investigated with numerical methods and the results are compared to experiments. It is shown how the aerodynamic performance depends on the design of the flow straightener in-between the fans and how this arrangement affects the acoustic behavior with respect to sound power and sound quality.

INTRODUCTION

Compact fans are often used to control the temperature of electronic devices, such as telecom base stations or large computer racks. In order to meet varying cooling demands various methods of control can be applied such as dampers, variable inlet vanes, variable blade pitch or variable fans speed [2] or combinations of these. To meet special constraints and increase system availability, fans are often installed in parallel and/or in series connection. A serial arrangement is advantageous in cases where high system pressure resistance must be overcome. Using two fans in series and operate them at same speed yields an increase of static the pressure of the staged fan system [3]. In this study, the effect of two identical compact fans in serial connection is studied with respect to air performance and noise generation. The noise generated depends on fan type, airflow rate and pressure. Inefficient fan operation is often indicated by a comparatively high noise level. Especially the second axial fan in the serial connection could generate a high noise level.

Beside the two fans, the arrangement in this study consist of flow straightening devices in-between the two fans. Various types of straighteners result in different pressure levels and airflow rates and also affect the noise level. The goal is to optimize air performance and minimize noise. For this purpose, the commercial flow solver Star-CCM+ V6.04.14 [9] has been used to compute the aerodynamic and aero acoustic behavior. In the later part of the paper a comparison of the numerically obtained aerodynamic performance to experiments is presented.

NUMERICAL MODEL

The numerical setup consists of two identical axial fans with flow straighteners in between, the inlet and outlet regions are placed sufficiently far upstream and downstream, respectively. The set-up is intended to model free inflow and outflow conditions of the test rig, as described in [8]. The rotor diameters are about 85mm, the total length of the entire fan setup is 97mm. Both fans are rotating in the same direction with a constant speed of 10500rpm. The blades and guide vanes of the first fan, the straightener and the blades and guide vanes of the second fan are each modeled as separate regions and framed by fully developed interfaces.

The inlet channel is defined as velocity inlet and the outlet as pressure outlet with p_{amb} = 101325 Pa. The fan performance has been computed for airflow rates from 175 m³/h to 315 m³/h. The rotation axis is the z-axis. The ambient temperature has been set to 300 K at constant density. The mesh is an unstructured polyhedral mesh with four million elements. The turbulence model is the standard k-ε model. In Figure 1 the computational domain and the unstructured polyhedral mesh structure including prism layers on surfaces are visualized.

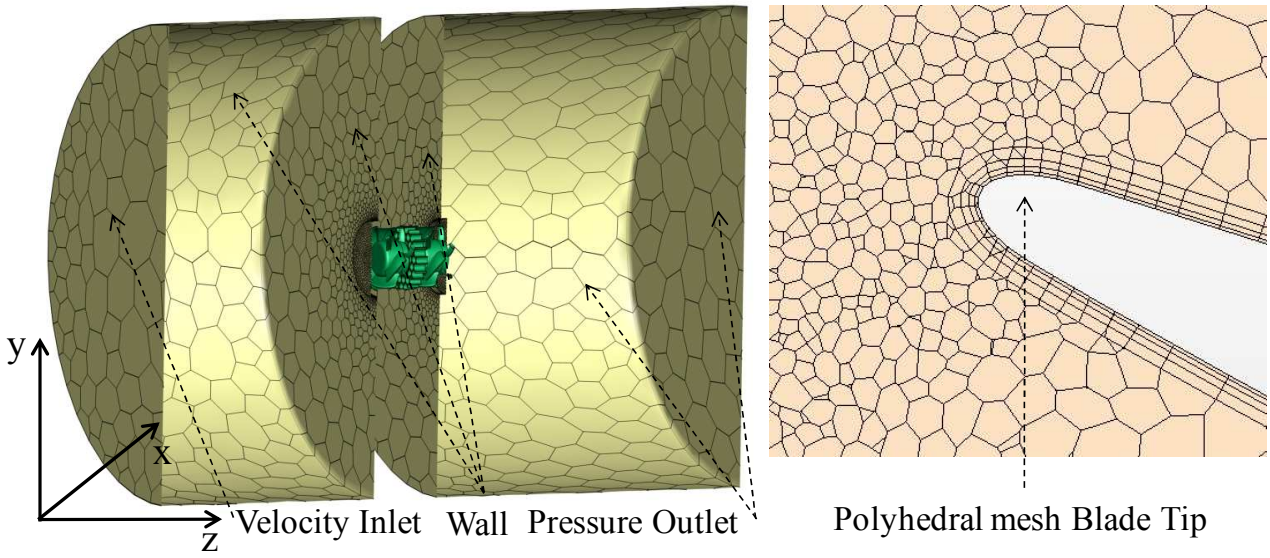

Figure 1: Computational domain

The reference values for meshing are given in Table 1. The given parameter ratios are calculated relative to a preliminary determined Base Size of 100 mm.

Table 1: Mesh parameters

Base Size [mm]	Nr. of Prism Lay.	Prism. Lay. Thick. ratio	Rel. Min. Size ratio	Target Size ratio
100	4	0.0026	0.001	0.045

The flow field is evaluated at eight planes normal to rotation axis and three blade-to-blade planes as illustrated in Figure 2. The overall pressure increase of the fan system is computed at the inlet and outlet of the computational domain, respectively.

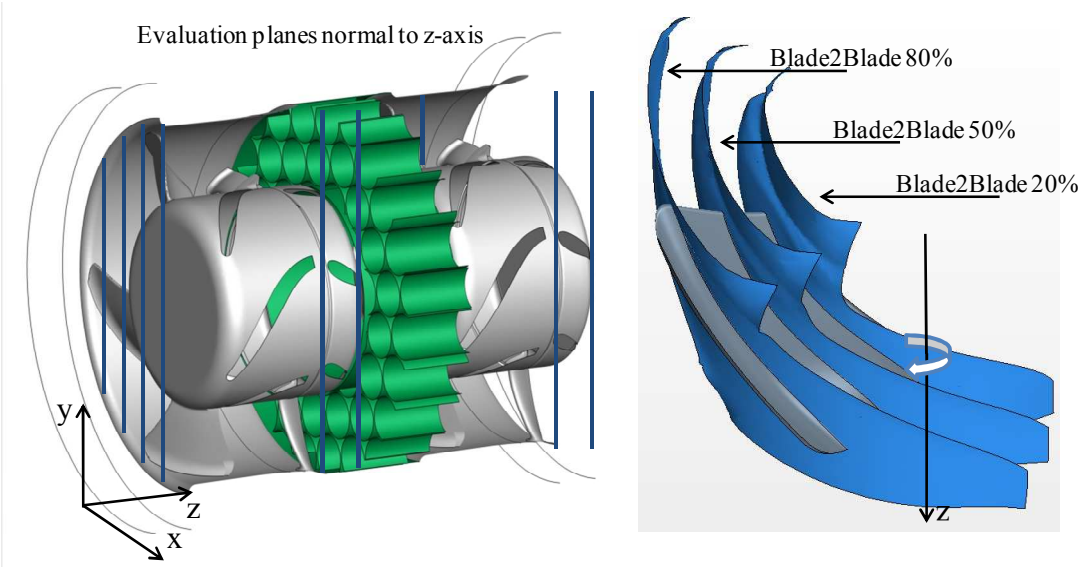

Figure 2: Evaluation planes

Two types of computations has been performed. A steady calculation using a frozen rotor approach and a fully unsteady computation with sliding mesh interfaces between the components. The solid lines in Figure 2 indicate also the locations of the interfaces.

AXIAL FANS IN A SERIES CONNECTION

A. Fan Arrangement

Figure 3 illustrates the fan set up with the flow straightener in between. In this study, mesh diameter (a), the axial depth (b) and the spacing between fans and straightener (c) have been varied (ref. Table 3).

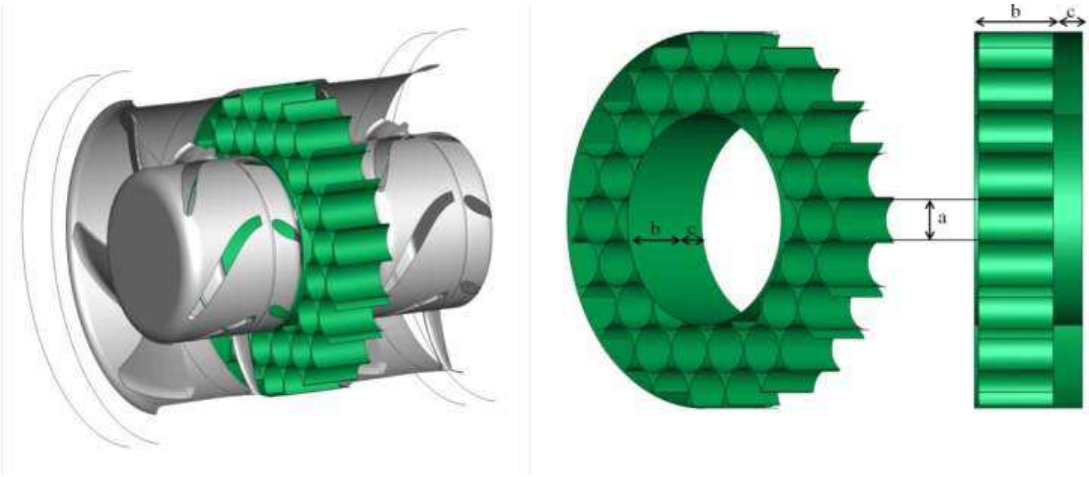

Figure 3: Example axial fans in a series connection & straightener

B. Experimental Set-Up

The aerodynamic test rig (Figure 4) is a suction side throttled facility according to ISO 5801. The test object is mounted at the test chamber exit; the inlet flow is conditioned with screens and gauzes to ensure homogeneous flow at the fan inlet. The air enters the rig via five tubes, each equipped with a flow meter. An auxiliary fan compensates the pressure drop in the system. The fan exit is at ambient, the static pressure difference in the inlet chamber against ambient is recorded.

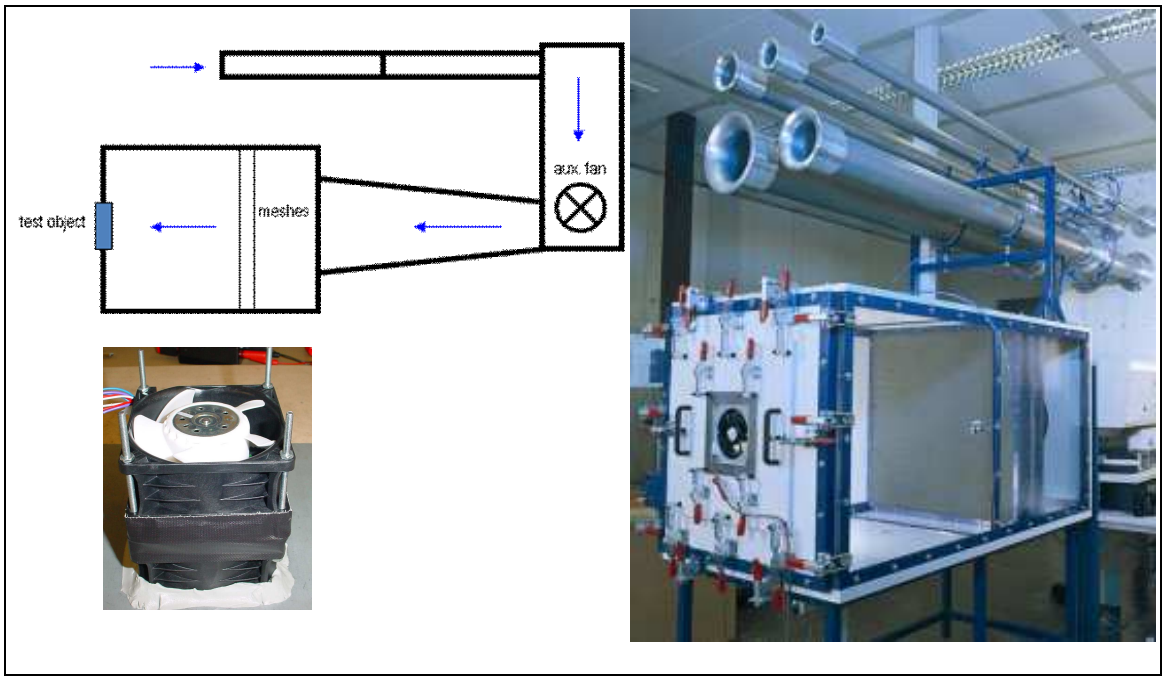

Figure 4: Experimental test set-up and test object.

In Table 2 the results of steady and unsteady simulations are compared in terms of static and total pressure rise, Δp_{fa} and Δp_t, and static and total efficiency, η_{fa} and η_t, with $\eta_{fa} = \frac{\Delta p_{fa} * \dot{V}}{2 * \pi * n * M_d}$ and $\eta_{fa} = \frac{\Delta p_t * \dot{V}}{2 * \pi * n * M_d}$, respectively. $\dot{V}$ denotes the fluid flow rate, n the rotation rate and M_d the aerodynamic torque. The calculated pressure rise of the transient calculation is about 6.9 % different to the frozen rotor model, while the efficiency values are about 4.2 % higher.

Table 2: Comparison of steady and unsteady simulation V=200 m3/h

Simulation Model	**Δpfa [Pa]**	**Δpt [Pa]**	**ηfa [%]**	**ηt [%]**
Frozen Rotor	733.0	733.4	46.8	46.8
Transient Rotor Stator	780.2	780.2	48.8	48.8
$\Delta_{\mathbf{Frozen}}$ **[%]**	6.4	6.9	4.2	4.2

For the purpose of this study, these differences are thought to be acceptable. Therefore, the frozen rotor model has been used for all further investigations in order to reduce computational effort and time. Figure 5 shows measured and the so calculated performance of a typical set-up (flow straightener diameter a = 12 mm, depth b = 18 mm; length c = 8 mm).

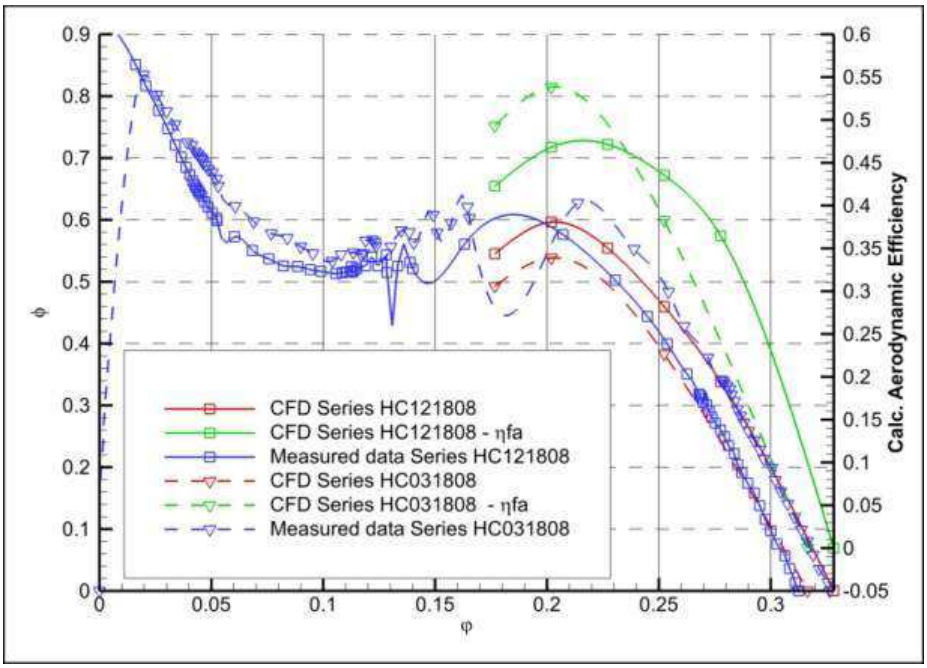

Figure 5: Performance map of two setups with wide and narrow straightener

C. Overall Loss Considerations

To assess the efficiency of a particular configuration, the total pressure increase at different positions along the axis is shown in Figure 6 for two different test cases. The influence of the mesh diameter of the straightener on the on the total pressure drop can be identified. This is the main reason why the stage with the narrow mesh reaches only 95% of the pressure rise of the stage with the wider straightener.

In most cases, the static pressure rise from inlet to outlet is a reasonable measure for the effectiveness of fans. Consequently, the mixing losses at the fan exit are included in this balance. Depending on this balancing scheme, the first fan can be considered to have higher efficiency than the second fan stage. This is particularly true when looking at the overall pressure increase of each fan. As in every multistage arrangement, the first fan stage does not have uncontrolled flow mixing and is not affected by the upstream effect of the downstream mixing flow as this is true for the second fan. The pressure drop over the stator row of the second fan is therefore higher as the pressure drop in the stator row of the first fan.

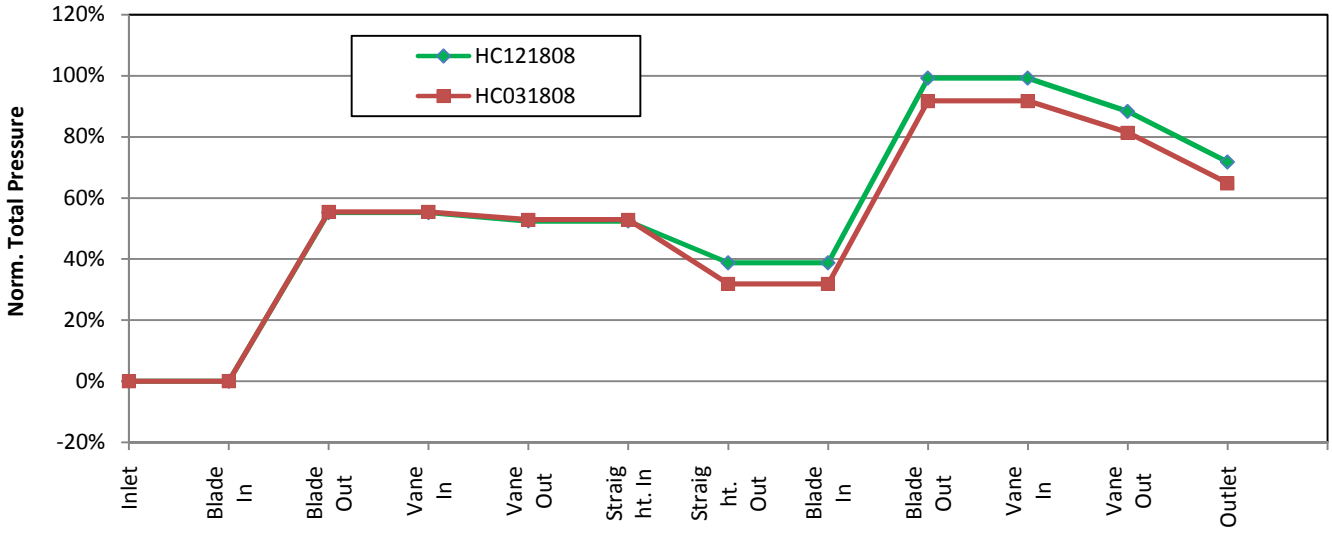

Figure 6: Relative total pressure increase along the axis

INFLUENCE OF STRAIGHTENER GEOMETRY

Nine variants of straighteners have been investigated with respect to flow performance and noise levels. Table 3 shows the parameter set-up of the analyzed straighteners. The notation HC031808 refers to a straightener with mesh diameter 3 mm, width of 18 mm and a spacing of 8 mm between straightener and leading edge of the second fan.

Table 3: Straightener types & geometric parameters

Straightener type: HC[diam.][depth][spacing] : HC[xx][xx][xx]			
Diameter (3 mm – 12 mm)	**HC031808**	**HC061808**	**HC121808**
Width (6 mm – 18 mm)	**HC120618**	**HC121208**	**HC121808**
Spacing (3 mm – 12 mm)	**HC121802**	**HC121808**	**HC121812**

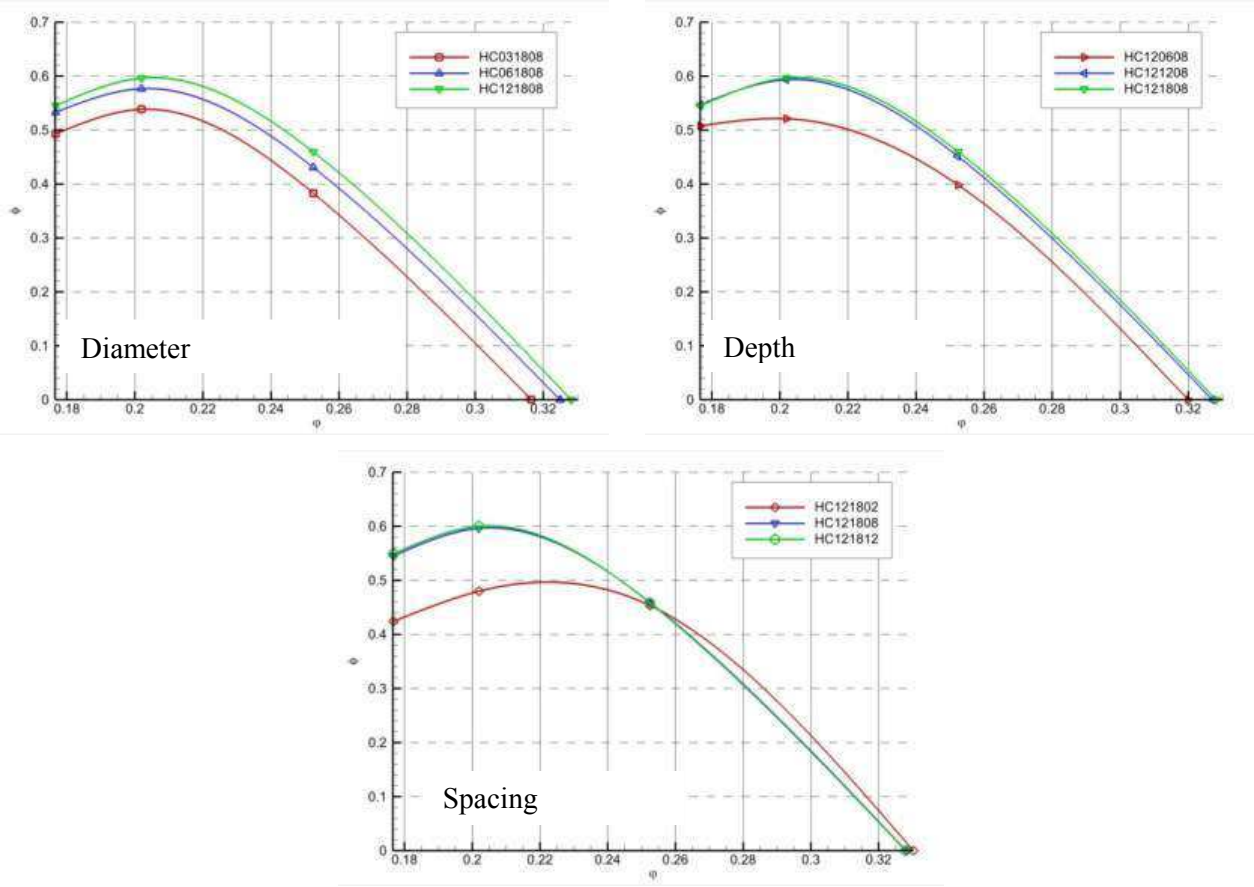

Figure 7: Performance map for different types of straighteners

According to Figure 7 (upper left), the mesh diameter affects the overall performance in terms of flow and pressure coefficient. The length of the straightener has a positive effect up to a limit (upper right picture). From there on, a further performance enhancement cannot be obtained. The same is true for the spacing of the components. Installing the fans too close to the straightener has a negative impact on the pressure coefficient (lower picture). In the next section, the flow field through the straightener is investigated in more detail.

FLOW FIELD ANALYSIS

In the following section, more in-depth analyses are presented. Two set-ups have been chosen with different flow straighteners. A set-up with a flow straightener having a mesh diameter of 12mm is compared to a straightener with 3mm mesh size. Both devices have 18mm width and a gap of 8mm up to the downstream fan stage (HC121808 vs. HC031808)

A. Rotor row of first fan

The velocity vectors are shown at 50% span height in Figure 8. The computed incidence angle is between one to nine degrees for both cases. According to Casey [7], the incidence of a compressor should be of the order of seven degrees for best operation. The downstream structure seems to have only small effect on the flow field of the first rotor row.

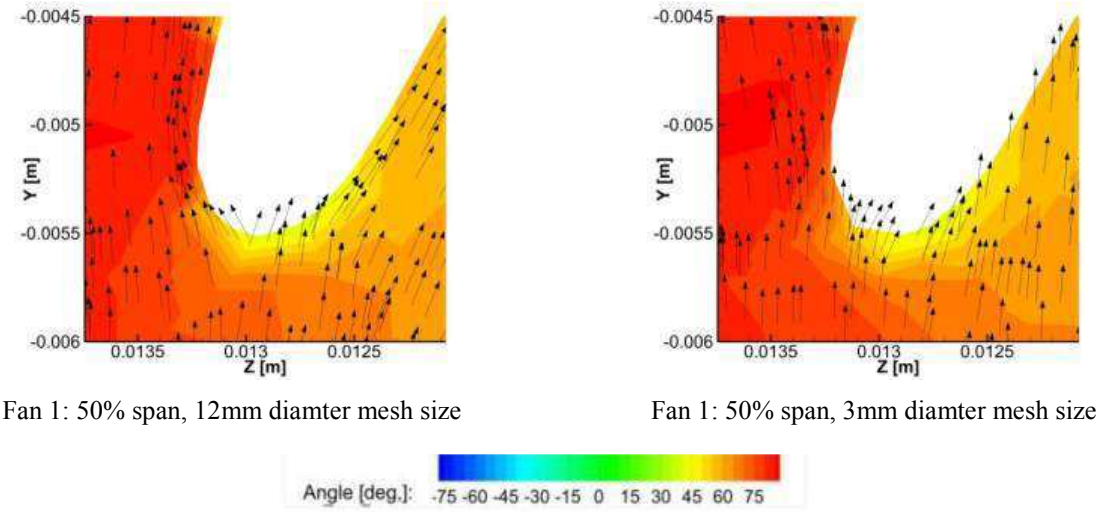

Fan 1: 50% span, 12mm diamter mesh size

Fan 1: 50% span, 3mm diamter mesh size

Figure 8: Velocity vectors at blade of fan 1

This is supported by the distribution of the gauge total pressure in the rotating frame of reference at 80% span height (Figure 9). The impact of the tip vortex on the pressure side of the blade is visible; however, the flow structure in both cases is very similar, indicating only small influence due to the different downstream straighteners.

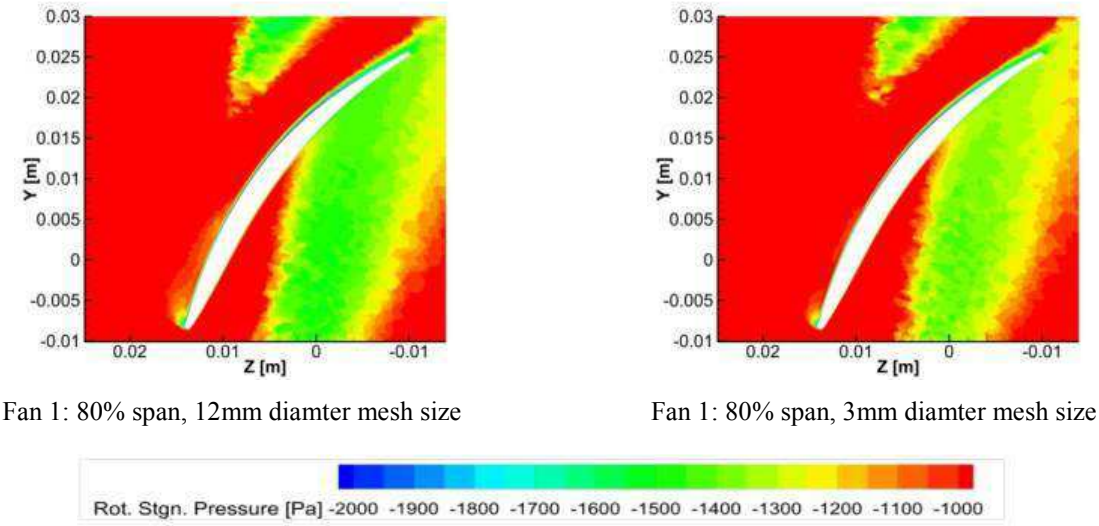

Fan 1: 80% span, 12mm diamter mesh size

Fan 1: 80% span, 3mm diamter mesh size

Figure 9: (Gauge) rotary stagnation pressure blade of first fan stage

B. Guide vanes of first fan

The guide vanes or struts of compact fans are mainly designed to minimize noise emission rather than recovering static pressure. Consequently, the design objective is to cause smallest turbulence and least flow obstruction. Figure 10 shows the value of the total pressure gradient as a measure for the locations with highest losses. Here, the differences in the flow field become visible. The narrow mesh causes a more homogeneous flow field of the vane. Therefore, this arrangement is expected to generate less noise than the one with the wider mesh.

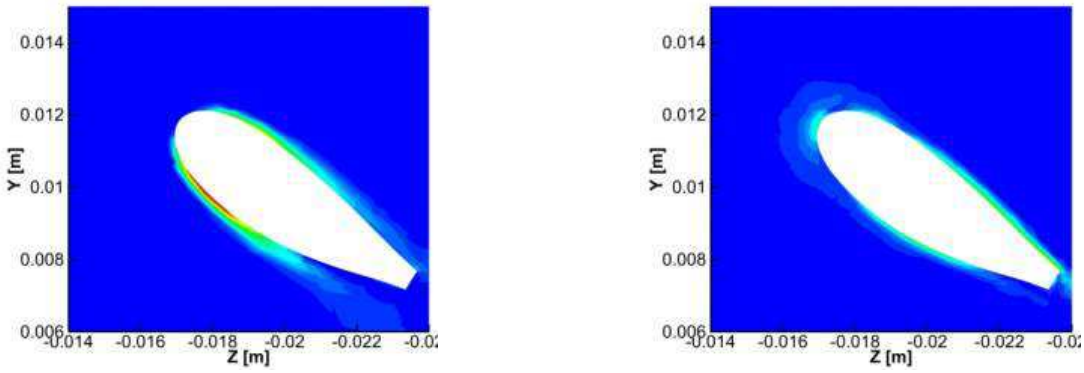

Fan 1: 50% span, 12mm diamter mesh size

Fan 1: 50% span, 3mm diamter mesh size

Figure 10: Total Pressure gradient along the guide vanes of the first stage.

C. Flow straightener

Figure 11 shows an axial cut through the flow straighteners and the corresponding flow field. The swirl downstream of the first stage causes high incidence angles to the straightener mesh, which in turn fosters the development of recirculation zones every cylindrical flow passage of the wider mesh (left picture). The straightener decreases the radial and circumferential velocity components, which increases the axial velocity [6], the overall flow rate increases. In Figure 11 the velocity magnitude through the straighteners are shown. The recirculation zones in the wider mesh blocks about 40% of the flow channel whereas for the narrow mesh no significant recirculation is computed. However, as shown in Figure 6 the total pressure losses of the narrow mesh are higher.

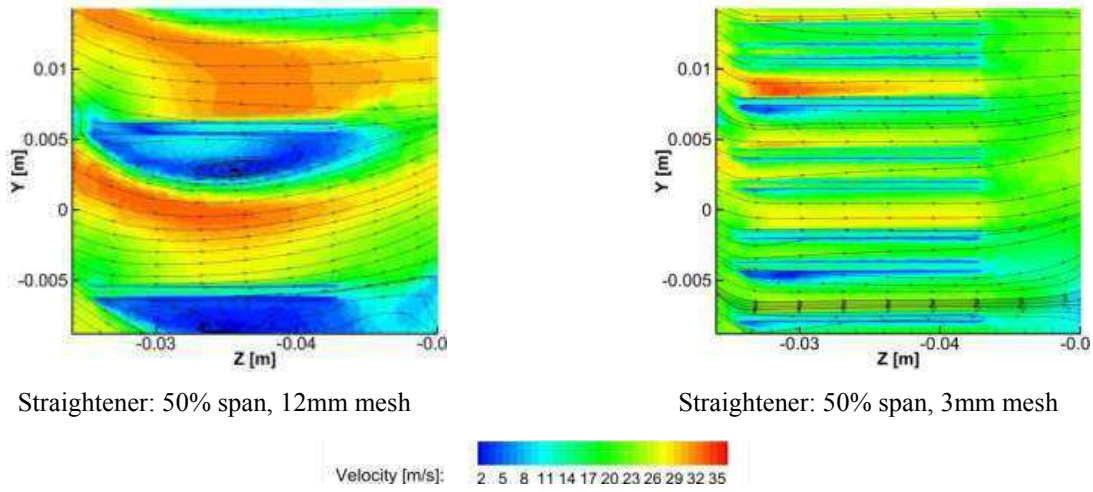

Straightener: 50% span, 12mm mesh

Straightener: 50% span, 3mm mesh

Figure 11: Velocity through flow straightener

The performance of the second fan stage depends on its inflow conditions, i.e. on the flow field at exit of the straightener. To accommodate for good performance, the flow field should be as homogeneous as possible. In Figure 12 the velocity gradient is shown at the entry of the second fan stage. Regions of high velocity are highlighted. Increasing mesh size results in stronger velocity

gradients and increasing noise level. For good acoustic behavior, a homogeneous flow pattern with small velocity gradients is desired.

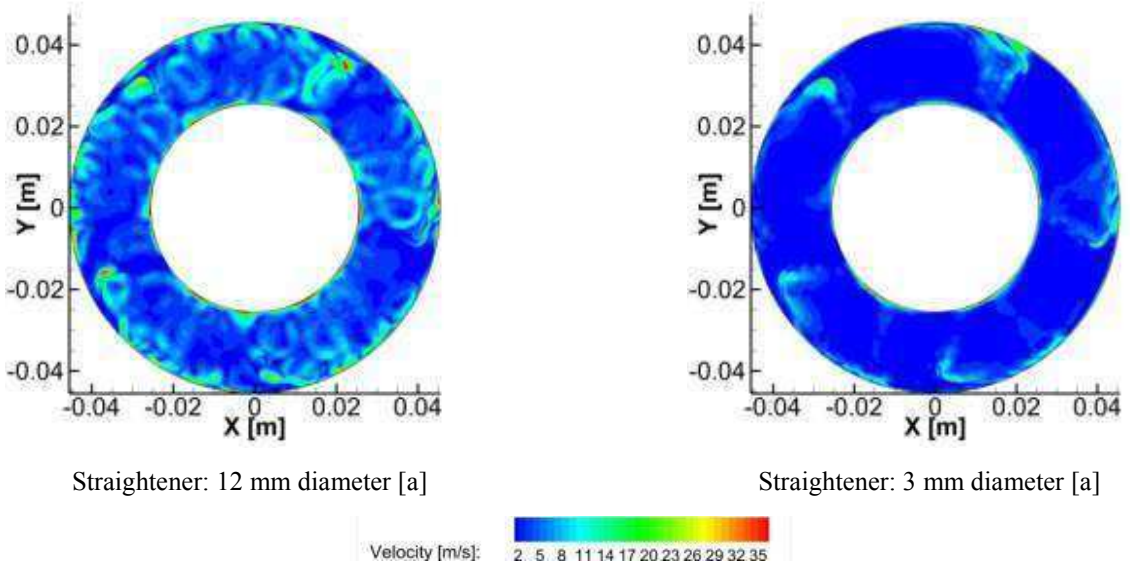

Straightener: 12 mm diameter [a] Straightener: 3 mm diameter [a]

Figure 12: Straightener: velocity at inlet of fan 2

D. Rotor row of second fan

The inflow conditions to the second fan stage are those of a ducted fan, in contrast to the first stage, which has free inflow conditions. The difference in the inflow conditions should be most visible at the blade tip. According to Figure 13 there is a shift in the location of the tip vortex compared to its position in the first fan stage. The higher turbulence intensity is thought to be the reason for increased mixing and therefore less sharply developed boundaries of the flow structure.

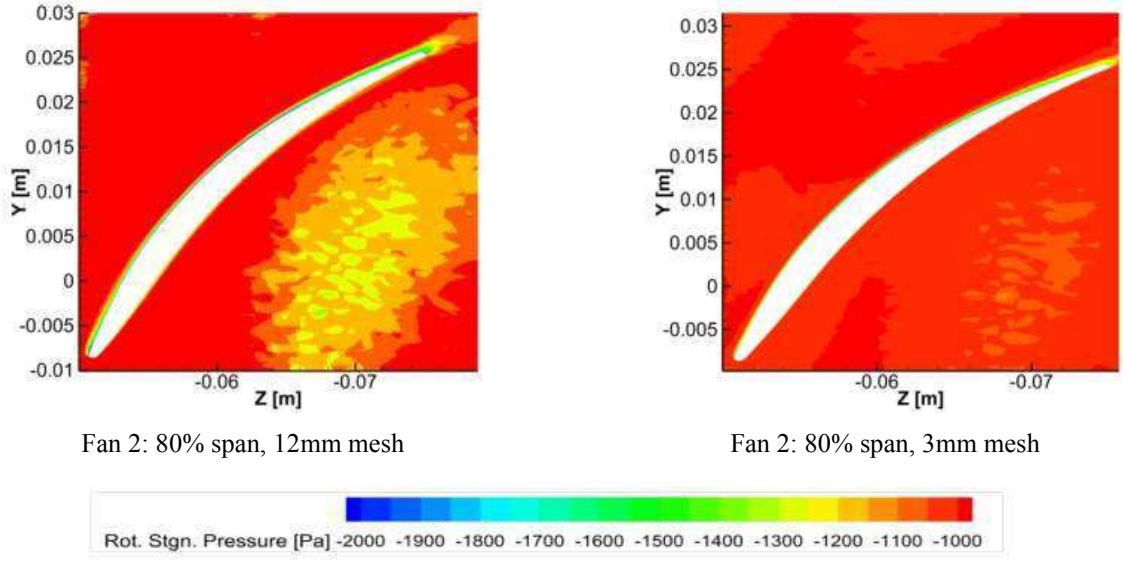

Fan 2: 80% span, 12mm mesh Fan 2: 80% span, 3mm mesh

Figure 13: (Gauge) rotary stagnation pressure at blade of fan 2

E. Guide vanes of second fan

A well-positioned flow straightener can cause similar flow through both fans. Comparing the flow to the guide vanes of the second stage (Figure 14) only small difference between the two fan stages can be found. The differences in the flow structure are caused by the different mesh diameters but not by a misalignment of the fans itself.

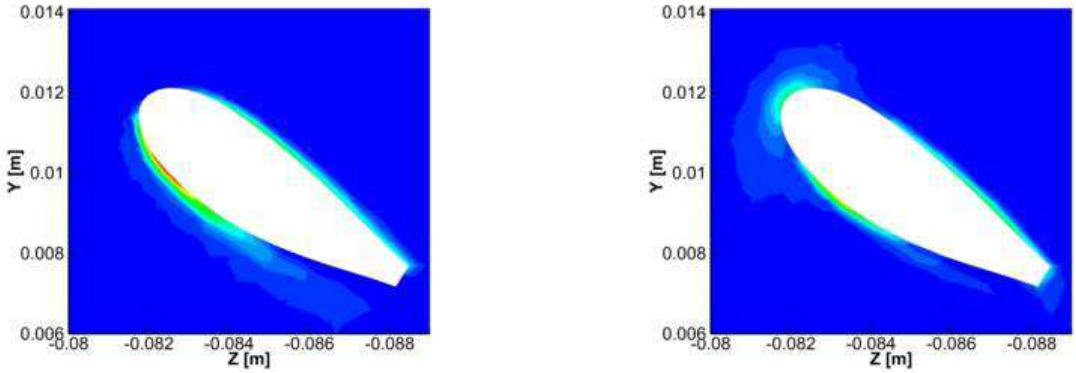

Fan 2: 50% span, 12 mm mesh

Fan 2: 50% span, 3 mm mesh

Figure 14: Total Pressure gradient along the guide vanes of the second stage

ACOUSTICS

To assess the acoustic behavior of the two-stage setup, the "Curle Surface Acoustic Power Model", has been used to calculate the acoustic dipole power on surfaces. Since at this stage of the project, no acoustic tests were available, the results of the calculation mainly were used to get indications of the relative behavior of the configurations. The Curle analogy is based on the same fundamental equations than Lighthill's analogy. Given a finite surface in a stationary system, the monopole sources on body surfaces and the dipole and quadrupole sources in fluid volume are getting to zero. The acoustic sound power P_{Dipole} for dipoles is calculated as [3]:

$$P_{Dipole} = \int_S I(y) dS(y) \,, \tag{1}$$

where *I(y)* is sound intensity and *dS(y)* is the surface area. The sound intensity *I(y)* is calculated as:

$$I(y) = \overline{p`^2} = \frac{1}{16\pi^2 \alpha_0^2} \int_S \frac{\cos(\theta)^2}{r^2} \overline{\left[\frac{\delta p}{\delta t}(y, t - \frac{r}{r_0}\right]^2} A_c(y) dS(y) \,, \tag{2}$$

The acoustic power per unit area can be written as:

$$P_{Dipole} = \int_S \frac{A_c(y)^2}{12\rho_0 \pi a_0^3} \overline{\left[\frac{\delta p}{\delta t}\right]^2} dS(y) \,, \tag{3}$$

where A_c is the correlation area and cos(θ) the angle between radius r of observer and the normal vector n of surface, α_0 is the velocity in the far field, r_0 the radius of observer in far field, p/p' the pressure/deviation pressure and ρ the density.

The aero acoustic results are shown in Figure 15 for the wide straightener mesh (HC121808) and the narrow mesh (HC031808). The highest sound power is generated at leading edges of the guide vanes and the tips of the blades. In Table 4 the results are listed.

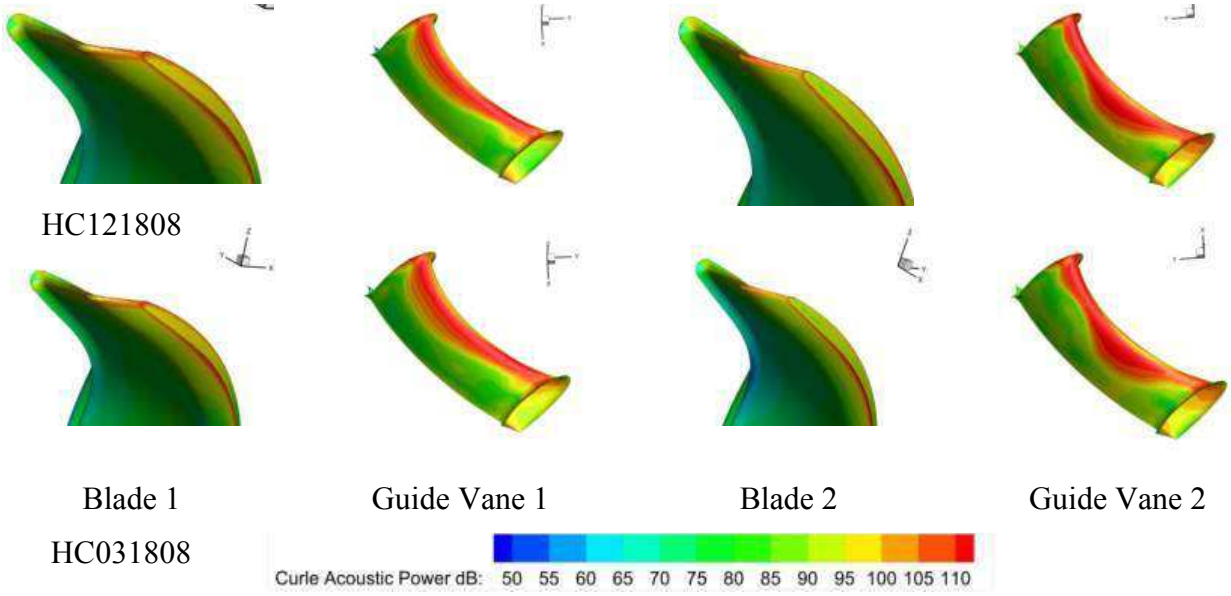

Figure 15: Aero acoustic dipole surface power [dB]

Table 4: Results Dipole Surface Power (12 mm straightener / 3 mm straightener)

Multipole	**Blades 1**	**Vane 1**	**Straight.**	**Blade2**	**Vanes 2**
Dipole [dB]:	95.0/95.0	82.4/82.2	71.7/72.1	95.8/95.2	83.8/83.0
Sum Dipole [dB]:	**98.7/98.3**				

According to the simulation, the second fan generates higher noise levels, especially on the guide vanes. Decreasing the mesh diameter of the straighteners leads to lower sound power levels, mainly in the second stage. Based on the investigation of all nine straighteners, the normalized results are presented in Figure 166. The geometric parameters are normalized with the rotor diameter and the acoustic power level is normalized to a source of 100 dB. The pressure increase is almost independent of the size of the spacing between straightener and second stage. The biggest impacts on flow performance have mesh diameter and depth of the straightener. The spacing has strong influence on the acoustic power level, while the width of the straightener and the mesh diameter are of minor influence.

Although the trend in the acoustic computation is reasonable, the differences in the actual values are very small. The results should be used with caveat and the authors do not state that this method, as applied, is a validated tool for reliable acoustic predictions. First acoustic experiments support the trend but also indicate a more significant impact on noise reduction of the narrow straightener. This has to be investigated in detail.

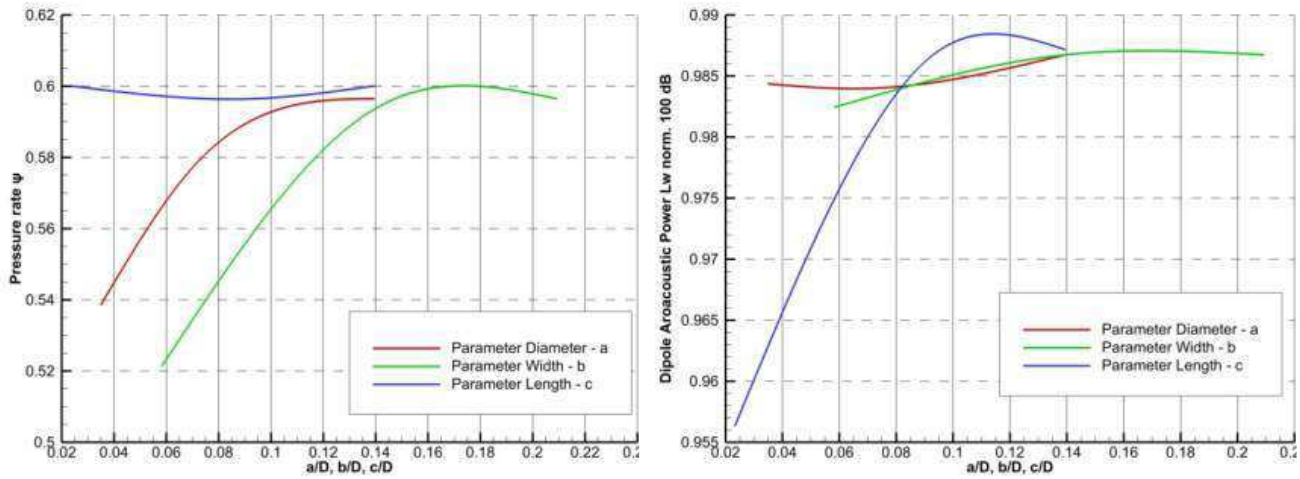

Figure 16: Normalized results straightener

CONCLUSION

The flow through a two-stage arrangement of identical compact fans with flow straighteners in between has been computed with 3D CFD. The investigation showed good comparison of the numerical calculations to experiments. The numerical flow field has been analyzed in more detail to identify and quantify the areas where the highest losses occur and to identify which components contribute most to the noise generation. The blades and guide vanes of the second fan have been found to be the biggest contributors to the overall sound power level. The different types of straighteners affect the performance and noise level. The mesh diameter and the width of the straightener have the strongest impact on the pressure rise of the system. For best noise level, a long flow channel after the straightener is advantageous. In this study, the best compromise regarding aero performance and noise level has been identified as a mesh diameter of 3mm, a straightener width if 18mm and a spacing of 8mm to the second stage. The acoustic computational methods is thought to deliver a reasonable trend, however a more detailed investigation and comparison to experiments has to be undertaken in the future.

REFERENCES

[1] T. Carolus – *Fans, Aerodynamic Design, Acoustics and Performance,* Vieweg, Teubner, **2003**

[2] A. Rangwala – *Control System Trends in Turbomachinery,* Anshan, **2011**

[3] L. Bommes –*Fans,* Vulkan, **2002**

[4] N. Curle – *The Influence of Solid Boundaries upon Aerodynamic Sound,* Proceedings of the Royal Society of London, **1955**

[5] I. Proudman – *The Generation of Noise by Isotropic Turbulence,* Proceedings of the Royal Society of London, **1952**

[6] D. Japikse – *Diffusor Design Technoloy,* Concepts ETI, Inc., **1998**

[7] M. Casey – *Basics of Turbomachinery,* ITSM University of Stuttgart, **2008**

[8] M. B. Schmitz, G. Eimer, H. Schmid – *Design and Test of A Small High Performance Diagonal Fan,* GT2011-45365, IGTI 2011, Vancouver, **2011**

[9] CD-Adapco, STAR-CCM+ Version 4.02 User's Manual **2009**.